

# Journal of Materials Chemistry C

Accepted Manuscript



This is an *Accepted Manuscript*, which has been through the Royal Society of Chemistry peer review process and has been accepted for publication.

*Accepted Manuscripts* are published online shortly after acceptance, before technical editing, formatting and proof reading. Using this free service, authors can make their results available to the community, in citable form, before we publish the edited article. We will replace this *Accepted Manuscript* with the edited and formatted *Advance Article* as soon as it is available.

You can find more information about *Accepted Manuscripts* in the [Information for Authors](#).

Please note that technical editing may introduce minor changes to the text and/or graphics, which may alter content. The journal's standard [Terms & Conditions](#) and the [Ethical guidelines](#) still apply. In no event shall the Royal Society of Chemistry be held responsible for any errors or omissions in this *Accepted Manuscript* or any consequences arising from the use of any information it contains.

# Electron Energy Level Engineering in $\text{Zn}_{1-x}\text{Cd}_x\text{Se}$ Nanocrystals

Kiran G. Sonawane,<sup>1,3</sup> Chinmay Phadnis,<sup>1</sup> Laxman Tatikondewar,<sup>1</sup> V. Sudarsan,<sup>2</sup> Anjali Kshirsagar,<sup>1</sup> and Shailaja Mahamuni\*<sup>1</sup>

Variation in composition provides additional degree of freedom in nanocrystals. In a strategic manner, amount of Zn across radius of  $\text{Zn}_{1-x}\text{Cd}_x\text{Se}$  nanocrystals (NCs) is varied which show minimal photoluminescence quenching with temperature, hence assuring the least defect density. Further Zn distribution within NCs is made uniform by annealing. Electron energy levels mapped by the optical techniques reveal reduced energy level spacing due to Zn incorporation. The Stokes shift attains remarkably lower value in alloyed  $\text{Zn}_{1-x}\text{Cd}_x\text{Se}$  NCs. Further, notable fact is that alloyed NCs concomitantly exhibit blue shift in the forbidden gap but red shift in higher energy transitions. First principles electronic structure calculations show enhanced hybridization of Zn *d* levels with Se *p* levels in comparison to that of Cd *d* levels in homogeneously alloyed NCs leading to decreasing energy difference between the occupied electron energy levels. Size variation tunes the optical transitions monotonically, while tuning the composition profile is capable of engineering the electron energy levels of NCs.

## 1. INTRODUCTION

The study of nanometer size semiconductors is rigorously initiated since last two decades. By the end of the previous century, control on the excitonic transition energy in semiconductor nanocrystals (NCs) due to quantum size effects was realized in various materials.<sup>1-4</sup> Variety of preparation routes emerged in due course of time with better control on the size, its dispersion and moreover on the shape.<sup>5</sup> Studies on core/shell NCs received special attention due to enhanced stability and improved luminescence efficiency.<sup>5-8</sup> Core/shell NCs are formed by overcoating smaller band gap semiconductor NCs, with another semiconductor having larger band gap. These hetero-nanocrystals suffer from the problem of interfacial defects and traps. Recent studies indicate that the interfacial defects and traps are optically active and are observed at low temperature.<sup>9-11</sup> Subsequent attempts to vary composition across radius of NCs was successful in minimising the lattice strain and hence the defects. Interestingly, composition

graded semiconductor quantum dots also show suppressed blinking in the single particle spectra.<sup>12</sup>

Composition variation across radius of NCs open up another degree of freedom to control the properties.<sup>13-16</sup> For example, radially alloyed NCs usually referred as “graded” core/shell structure exhibit a superior PL efficiency as compared to normal core/shell NCs.<sup>13-14</sup> In these radially alloyed or graded NCs, composition is continuously varied from core to shell to obtain a core/shell structure. Effectively defect free NCs could be obtained by graded composition.<sup>17</sup> Some properties, like blue emission in CdSe, is possible only by reducing the size, which almost always leads to increased defect density in NCs.<sup>17</sup> This problem can be overcome in case of uniform alloy with homogeneous composition throughout the NCs. The main strategy to synthesize alloyed NCs involve synthesis of core/shell structure and annealing them at particular condition to cause diffusion.<sup>18</sup> Another strategy to form an uniform alloy is cation exchange reaction in pre-formed nanocrystals.<sup>19-21</sup> The graded alloy or core/shell structure can be produced by utilizing the difference in reactivity of precursors.<sup>22-23</sup> However, initially graded core/shell structure, can be annealed to form homogeneous alloy structure. This approach reduces the interfacial defects that are prone to present in core/shell structure, which will affect the quality of final alloyed structure. In this paper, same idea is explored to generate graded core/shell structure and homogeneous alloy structures.

Although the change in band gap with composition is discussed in the literature,<sup>17-24</sup> the electron energy levels of NCs with varying composition across the radius are not unravelled. In the present report, composition graded and alloyed  $Zn_{1-x}Cd_xSe$  NCs grown by single pot method are studied. This paper discusses the evolution of electron energy levels from graded to homogeneous alloy. Electron energy levels are mapped using photoluminescence excitation

(PLE) spectroscopy. The evolution of excited state energy levels from graded to alloyed  $Zn_{1-x}Cd_xSe$  NCs, are understood on the basis of first principles electronic structure calculations using pseudopotential based plane wave method. The comparison enabled us to understand blue shift in the forbidden gap and red shift in higher optical transitions in alloyed NCs. The present findings are useful in designing the advanced semiconductor with increased forbidden gap and reduced, perhaps even metallic like electron energy level spacing.

## 2. METHODOLOGY

**(a) Experimental:** Graded  $Zn_{1-x}Cd_xSe$  NCs were prepared by chemical route reported elsewhere.<sup>14</sup> In a typical synthesis zinc acetate dihydrate, cadmium acetate dihydrate, oleic acid (OA), and octadecene (ODE) were mixed and heated to 300 °C, under inert atmosphere. A solution of Se trioctylphosphine and ODE was swiftly injected. The reaction solution is annealed for different time duration to produce graded core/shell and alloyed NCs. Because of different reactivity of Zn and Cd precursor with trioctylphosphine-Se (TOP-Se) complex, graded core/shell structure with CdSe rich core and ZnSe rich shell is formed.<sup>14</sup> Note that even though these NCs are called graded core/shell they are alloyed NCs with radially varying composition. The concentration of Cd is checked using inductively coupled plasma atomic emission spectroscopy (ICP-AES). For 25 % Cd in reaction solution actual concentration of Cd in sample is 36 % (ZnCdSe-I). Homogeneous alloyed NCs were grown by annealing the graded structure in chemical bath. Aliquots are taken for ZnCdSe-I at different reaction time viz. 30 minutes (ZnCdSe-Ia), 60 minutes (ZnCdSe-Ib), 120 minutes (ZnCdSe-Ic), and 180 min (ZnCdSe-Id). Annealing in chemical bath facilitate diffusion of Zn from the shell region to the core region. At this juncture, it may be noted that the  $Zn_{1-x}Cd_xSe$  NCs are prepared by single pot, high

temperature method in the present case. Thereby possibility of defect generation would be minimal compared to the reported work. Details on growth mechanism and alloy formation process can be found elsewhere.<sup>14</sup>

Optical absorption measurements were performed using Perkin Elmer lamda 950 spectrophotometer. PL and PLE at room temperature (RT) and 10 K are recorded with assembled PL setup. PL setup has Jobin-Yvon 450 W Xe lamp as source, TRIAX 180 monochromator as excitation monochromator, iHR 320 as emission monochromator, a photomultiplier tube, and Janis CCS 150 optical cryostat. Time resolved photoluminescence (TRPL) measurements were carried on Edinburgh Instruments, FLSP920 system. Sample is excited with nanosecond flash lamp operating with 6.8 kV voltage and 40 kHz pulse frequency. ICP-AES measurements were carried out on Spectra Arcos spectrometer.

**(b) Computational:** The electronic structure calculations are carried out within a supercell approach in k-space using projected augmented wave (PAW)<sup>25</sup> formalism as implemented in VASP package<sup>26</sup> for a fixed geometry of the NCs. The NCs are positioned at the centre of a large cubic unit cell (supercell) such that the minimum vacuum region from the surface of the NC to cell boundary is 3Å. The electronic charge density of the NCs approaches zero within this distance. The Brillouin zone (BZ) for this large unit cell is small enough to be sampled by just one k-point, the centre of the BZ. For calculating the atomic energy levels, the atom is placed at the centre of the supercell of size 15Å and calculations are performed in k-space only with same pseudopotential so that all the calculations are consistent. The plane wave cut off used is 465 eV, convergence criteria for energy for supercell calculations is  $10^{-4}$  eV. The electronic configurations used for Cd, Zn, and Se are  $4d^{10} 5s^2$ ,  $3d^{10} 4s^2$ , and  $5s^2 5p^4$  respectively. The PBE exchange-correlation energy functional used is used<sup>27</sup> in the calculations.

### 3. RESULTS AND DISCUSSION

Room temperature optical absorption and PL spectra of graded core/shell, and alloyed  $\text{Zn}_{1-x}\text{Cd}_x\text{Se}$  NCs are shown in Fig. 1. Absorption feature of these NCs is located at lower energy than bulk  $\text{ZnSe}$ ,<sup>28</sup> implying that  $\text{ZnCdSe-I}$  NCs are more or less  $\text{CdSe}$  like. As  $\text{Cd}$  is more reactive than  $\text{Zn}$  toward  $\text{TOP-Se}$ ,<sup>24,29,30</sup>  $\text{Cd}$  is anticipated to react fast, resulting in  $\text{CdSe}$  seed formation. Subsequently,  $\text{Zn}$  ions participate in the reaction to form a graded structure with  $\text{CdSe}$  rich core and  $\text{ZnSe}$  rich shell.<sup>14</sup> Actual composition of NCs is probed by ICP-AES and the results are discussed elsewhere<sup>14</sup>. The ICP-AES data clearly indicate formation of a graded structure with  $\text{CdSe}$  rich core and  $\text{ZnSe}$  rich shell. The graded NCs show PL efficiency of 60 %. Such a high efficiency indicates effective passivation of cationic and anionic site without interfacial defects.<sup>31-34</sup>

In order to facilitate diffusion of ions, sample is annealed. Annealing graded nanostructure at  $290^\circ\text{C}$  for longer time duration, typically up to 180 minutes yields<sup>14</sup> uniform alloy NCs. Alloy formation is confirmed by ICP-AES and x-ray photoelectron spectroscopy measurements.<sup>14</sup> Fig. 1 depicts absorption and PL spectra (recorded at RT) of the annealed NCs. Annealing causes blue shift in the absorption feature from  $539 \pm 5$  nm ( $2.3 \pm 0.02$  eV) to  $498 \pm 5$  nm ( $2.49 \pm 0.02$  eV). Concomitant blue shift in PL spectra is also observable from  $547 \pm 5$  nm ( $2.26 \pm 0.02$  eV) through  $501 \pm 5$  nm ( $2.48 \pm 0.02$  eV). Such a blue shift in band edge, without reduction in size, indicates formation of alloy structure (Fig. S1, Table S1). Further blue-shift is not observed in PL spectra after time duration of 180 min. Annealing NCs cause diffusion of  $\text{Zn}$  from shell in to  $\text{Cd}$  rich core and out diffusion of  $\text{Cd}$  in the shell region. The overall process results in formation of alloy, thereby blue shifting the band edge by 41 nm (189 meV). PL measurements reveal slight reduction in quantum efficiency on alloy formation. Even after alloy

formation PL quantum efficiency is  $\sim 45\%$ . Such a high efficiency is comparable to conventional core/shell structure, and is rare in alloyed or normal semiconductor NCs and hence assures defect free NCs. Progressive alloy formation leads to decrease in the Stokes shift (from  $8 \pm 1$  to  $3 \pm 1$  nm,  $33 \pm 4$  to  $15 \pm 4$  meV). Major contribution to Stokes shift is due to the exchange interaction between electron and hole in NC and decreases<sup>8,35,36</sup> with increasing size. Exchange interaction splits the lowest energy level into two levels with net spin projection  $J=1$  and  $2$ . Energy level with net spin projection  $J=2$  is optically forbidden and called as dark state whereas level with spin projection  $J=1$  is optically active and called as bright state. The difference in these levels leads to Stokes shift in NCs. Here, Stokes shift reduces as one increases concentration of Zn in the core. The reduced Stokes shift in alloyed NCs implies the reduction in dark and bright gap.

To analyze the effect of Zn incorporation on energy levels, PL and PLE measurements are carried out at 10 K. Fig. 2(a) shows PL spectra of ZnCdSe-I NCs recorded at 10 K. Blue shift ( $\sim 15$ - $19$  nm) in emission maxima is observed at low temperature (10 K). The blue shift is consistent with the dependence of band edge on temperature. Recent studies revealed that surface and interfacial traps are optically active and show their presence in low temperature PL spectra.<sup>9-</sup>  
<sup>11</sup> From Fig. 2(a) it is clear that at low temperature no extra feature other than band edge emission is observed for both graded and alloyed NCs. This supports our claim that the NCs are almost free of interfacial defects. Fig. 3(a) depicts PL emission peak intensity as a function of temperature. In case of graded NCs, PL intensity does not show appreciable quenching which is in contrast with the alloy NCs and hence further confirming negligible density of interfacial defect states along with localization of charge carriers at the centre of the NCs in graded sample.

It is worth noting here that even though particle size (ZnCdSe-I) is  $\sim 4.3$  nm, optical absorption of these NCs (ZnCdSe-I) matches with that of CdSe NCs with nominal size of  $3.2$

nm. Similarly PLE spectra also match with 3.2 nm size CdSe NCs (Fig. S2). This is a manifestation of the fact that emission is from core CdSe. However exact deduction of core size is not possible as exciton confinement inside NCs strongly depends on the shape of confinement potential.

Fig. 3(b) gives variation in PL emission energy as a function of temperature for graded (ZnCdSe-I) NCs which is quite different than that of alloy (ZnCdSe-Id) NCs. The temperature dependence of emission energy can be fitted by empirical Varshni equation [ $E_g(T) = E_g(T=0) - \alpha T^2/(T + \beta)$ ],<sup>37-41</sup> in order to estimate the difference quantitatively. The effect of size on  $\alpha$  and  $\beta$  parameters is studied on ZnSe and CdSe materials, in literature, and found not to depend on size of NCs. Here  $\alpha$  and  $\beta$  values for graded NCs are  $\alpha = 3.4 \times 10^{-4}$  eV/K and  $\beta = 225$  K (which are close to that of CdSe  $\alpha = 2.8 - 4.1 \times 10^{-4}$  eV/K and  $\beta = 181 - 315$  K).<sup>40</sup> One may thus conclude that the emission in graded (ZnCdSe-I) is from CdSe rich core. On the other hand,  $\alpha = 6.9 \times 10^{-4}$  eV/K and  $\beta = 330$  K for alloy NCs, deviate from that of CdSe and are close to that of ZnSe ( $\alpha = 6.9 \times 10^{-4} - 7.7 \times 10^{-4}$  eV/K and  $\beta = 260 - 330$  K ).<sup>39</sup> Such a change in  $\alpha$  and  $\beta$  parameters is observed in alloyed sample.<sup>39, 41</sup> One may thus conclude that in ZnCdSe-Id, the emission is truly from alloyed NCs.

The electron energy levels are extracted from PLE and assigned as in CdSe.<sup>1</sup> Fig. 2(b) shows the variation in energy levels as a function of annealing time. With increasing annealing time, difference between adjacent energy levels progressively decreases. Subsequently, energy levels of alloyed NCs are located closer to each other. Energy level spacing and forbidden gap in NCs increases as size is reduced.<sup>1</sup> Here, particle size of NCs is almost same, even though energy levels comes closer to each other and forbidden gap increases with Zn incorporation in the core. The increase in band gap is a property of smaller NCs. While reduced spacing in the energy

levels is a property of larger NCs. Alloyed NCs combine both the properties of smaller and larger NCs. The present experimental findings thus identify spatial distribution of composition as the parameter to engineer the physical properties of NCs. The variation in the microscopic composition of the NCs is changing the energy level spacing. Just like the excited state, the composition might also be changing the dark bright energy gap, which in turn is reducing the Stokes shift for alloyed NCs.

Fig. 4 depicts TRPL spectra of graded and alloyed NCs. Alloying is responsible for shortening PL life time while single exponential nature of the radiative decay is retained. These observations are suggestive of high quality of the NCs in terms of minimal interfacial defects.

In order to understand the origin of reduction in energy level spacing, first principles electronic structure calculations are performed. Geometries of  $\text{Zn}_{1-x}\text{Cd}_x\text{Se}$  NCs with Cd atom at the centre are generated<sup>42</sup> using the structural information available from experiments. For a fixed concentration of Cd, three possible arrangements of atoms at cation site are considered namely (i) core consisting of CdSe and shell consisting of ZnSe (core/shell structure), (ii) smaller core of CdSe, thinner shell of ZnSe, and middle region consisting of  $\text{Zn}_{1-x}\text{Cd}_x\text{Se}$  with progressively increasing concentration of Zn (graded structure), (iii) Zn and Cd atoms randomly occupying cation positions anywhere in NC (alloy structure). Calculations are performed for different sizes of NCs and various values of  $x$ . Here we report results for NCs of size 2 nm diameter and  $x=0.24$  (close to experimental concentration of 0.36). The dangling bonds on the surface atoms are satisfied using fictitious  $\text{H}^*$  atoms as passivating ligands.<sup>43</sup> We have earlier reported symmetry locking on passivation<sup>44</sup> hence results for a given geometry, without relaxation, are reported.

Detailed analyses of density of states (DOS) and partial charge densities of the orbitals predominantly responsible for transitions within the one-electron picture described by density functional theory are carried out. The highest occupied molecular orbital (HOMO) is mainly contributed by the Se *p* states and is localized in the central region of the NC, irrespective of the different arrangements of atoms as described above. (see Fig. 5). The bonding in these NCs is partly ionic and partly covalent. Few more orbitals below the HOMO level are Se *p* like indicating almost completely occupied Se *p* states hybridized with the cationic ***p*** and ***d*** states. Partial charge density of lower levels extends spatially outwards in comparison to HOMO partial charge density. Lowest unoccupied molecular orbital (LUMO) states consist of cation *s* states hybridized with Se *s* and *p* states. It is seen that the partial charge density of LUMO level is spread all over the NC in case of core/shell structure while it shrinks toward the centre in alloy structure (Supplementary Information Fig. S3). This clearly manifests enhanced hybridization of Se states with Zn states compared to Cd states. The enhanced hybridization of Zn with Se in comparison to Cd can be understood from energy levels of individual atoms (Supplementary Information, Fig. S4 and S5). As is evident Zn *s* and *d* levels are closer to Se *p* levels in comparison to Cd *s* and *d* levels respectively. Thus the hybridization in HOMO and lower levels will be dominated by the Zn atoms in arrangement (ii) and more so in (iii). This explains reduced spacing in higher energy transitions in alloyed NCs. On annealing, Zn atoms move toward the centre of the NC, the overlap of Zn *p* and *d* and Se *p* increases and splitting of bonding and antibonding states decreases. DOS plots also indicate that next group of lower states moves to lower energy values (Fig. 6). Since the calculations are carried out within the density functional theory approach, it is not possible to assign the experimentally observed transitions with single particle levels. The observed pattern in the experimental spectra can however be explained on the

basis of difference in the degree of hybridization of the states originating from the cations and  $p$  states of Se.

#### 4. CONCLUSIONS

The electron energy levels of high-quality, compositionally graded  $\text{Zn}_{1-x}\text{Cd}_x\text{Se}$  NCs are determined by optical spectroscopy. NCs show single photoluminescence decay curve and moreover, temperature induced quenching is absent. These findings ensure minimal defects in NCs which is a manifestation of single pot synthesis route. Progressive incorporation of Zn in core region results into reduced energy difference in higher transitions along with blue shift in forbidden gap. First principles calculations performed on prototype  $\text{Zn}_{1-x}\text{Cd}_x\text{Se}$  NCs shed light on the underlying phenomena. The calculations indicate enhanced hybridization of Zn levels with Se levels compared to those of Cd levels. Subsequently, energy spacing between occupied energy levels reduces with Zn incorporation in the core region. The partial charge density of HOMO level is spatially confined in the core region irrespective of the composition profile of NCs, while partial charge density of LUMO progressively shrinks towards the centre with alloying. Interestingly reduction is also observed in Stokes shift of alloyed NCs as compared to graded NCs.

Size variation provides a tool to tune the optical transitions monotonically. However, present findings clearly demonstrate electron energy level engineering by tuning the composition profile of NCs. To the best of our knowledge, this is the first report indicating feasibility of tuning higher energy transitions by varying composition in NCs. These findings are useful to design an advanced semiconductor with desirable forbidden gap and metallic like close electron energy level spacing.

## ACKNOWLEDGEMENTS

KGS, and CP, thank CSIR India, and DST India respectively for the financial support. LT thanks UGC through UPE nanomission, for the funding. Authors are also thankful to D.S.T. Unit on Nanoscience, CNQS and D.S.T. FIST program for various characterization facilities. AK thanks DST nanomission for financial support and C-DAC Pune for HPC facilities.

## Notes and References

<sup>1</sup>Department of Physics, University of Pune, Pune 411 007, India

<sup>2</sup>Chemistry Division, Bhabha Atomic Research Centre, Trombay, Mumbai 400 085, India

<sup>3</sup>CEES Department, MIT College of Engineering, Kothrud, Pune 411038, India

Corresponding Author: [shailajamahamuni@yahoo.co.in](mailto:shailajamahamuni@yahoo.co.in)

Electronic Supplementary Information Available: Details of particle size, energy levels extraction from PLE, LUMO partial charge density, and energy levels of individual Cd, Se, and Zn atom is discussed in Supplementary information. See DOI:

- 1 D. J. Norris and M. G. Bawendi, *Phys. Rev. B*, 1996, **53**, 16338.
- 2 D. J. Norris, A. L. Efros, M. Rosen and M. G. Bawendi, *Phys. Rev. B*, 1996, **53**, 16347.
- 3 V. V. Nikesh, A. D. Lad, S. Kimura, S. Nozaki and S. Mahamuni, *J. Appl. Phys.*, 2007, **101**, 103906.
- 4 M. Medeiros-Reibeiro, D. Leonard and P. M. Petroff, *Appl. Phys. Lett.*, 1995, **66**, 1767.
- 5 P. Reiss, *New J. Chem.*, 2007, **31**, 1843.

- 6 X. Peng, M. C. Schlamp, A. V. Kadavinich and A. P. Alivisatos, *J. Am. Chem. Soc.*, 1997, **119**, 7019.
- 7 B. O. Dabbousi, J. Rodriguez-Viejo, V. F. Mikulec, J. R. Heine, H. Mattoussi, R. Ober, K. F. Jenson and M. G. Bawendi, *J. Phys. Chem. B*, 1997, **101**, 9463.
- 8 M. A. Hines and P. Guyot-Sionnest, *J. Phys. Chem. B*, 1998, **102**, 3655.
- 9 J. Mooney, M. M. Krause, J. I. Saari and P. Kambhampati, *Phys. Rev. B*, 2013, **87**, 081201(R).
- 10 M. M. Krause, J. Mooney and P. Kambhampati, *ACS Nano*, 2013, **7**, 5922.
- 11 J. Mooney, M. M. Krause, J. Saari and P. Kambhampati, *J. Chem. Phys.*, 2013, **138**, 2014705.
- 12 X. Wang, X. Ren, K. Kahen, M. A. Hahn, M. Rajeswaran, S. Maccagnano-Zacher, J. Silcox, G. E. Gragg, A. L. Efros and T. D. Krauss, *Nature*, 2009, **459**, 686.
- 13 P. K. Santra, R. Viswanatha, S. M. Daniels, N. L. Pickett, J. M. Smith, P. O'Brien and D. D. Sarma, *J. Am. Chem. Soc.*, 2009, **131**, 470.
- 14 K. G. Sonawane, K. R. Patil and S. Mahamuni, *J. Lumin.*, 2013, **135**, 154.
- 15 A. Belabbes, M. Ferhat, M. And A. Zaoui, *Appl. Phys. Lett.*, 2006, **88**, 152109.
- 16 X. Lu, D. A. Beaton, R. B. Lewis, T. Tiedje and Y. Zang, *Appl. Phys. Lett.* 2000, **95**, 041903.
- 17 M. D. Regulacio and M. Han, *Acc. Chem. Res.*, 2010, **43**, 621.
- 18 X. Zhong, M. Han, Z. Dong, T. J. White and W. Knoll, *J. Am. Chem. Soc.*, 2003, **125**, 8589.
- 19 Y. Zeng, Z. Yang and J. Y. Ying, *Adv. Mater.*, 2007, **19**, 1475.
- 20 X. Zhong, Y. Feng, Y. Zhang, Z. Gu and L. Zou, *Nanotechnol.*, 2007, **18**, 385606.
- 21 X. Zhong, Z. Zhang, S. Liu, M. Han and W. Knoll, *J. Phys. Chem B*, 2004, **108**, 15552.

- 22 M. W. DeGroot, K. M. Atkins, A. Borecki, H. Rosnerb and J. F. Corrigan, *J. Mat. Chem.*, 2008, **18**, 1123.
- 23 W. K. Bae, K. Char, H. Hur and S. Lee, *Chem. Mater.*, 2008, **20**, 531.
- 24 H. Lee, P. H. Holloway, H. Yang, L. Hardison and V. D. Kleiman, *J. Chem. Phys.*, 2006, **125**, 164711.
- 25 P. E. Blochl, *Phys Rev. B*, 1994, **50**, 17953.
- 26 G. Kresse, J. Furthmuller, *Phys. Rev. B*, 1996, **54**, 11169.
- 27 P. Perdew, K. Burke and M. Ernzerhof, *Phys. Rev. Lett.*, 1996, **77**, 3865.
- 28 A. V. Nurmikko and R. L. Gunshor, *J. Lumin.*, 1992, **52**, 89.
- 29 (a) A. Nag, A. Kumar, P. P. Kiran, S. Chakraborty, G. R. Kumar and D. D. Sarma, *J. Phys. Chem. C*, 2008, **112**, 8229 (b) H. Liu, J. S. Owen and A. P. Alivisatos, *J. Am. Chem. Soc.*, 2007, **129**, 305.
- 30 M. Portiere and P. Reiss, *Small*, 2007, **3**, 399.
- 31 D. V. Talapin, A. L. Rogach, A. Kornowski, M. Haase and H. Weller, *Nano Lett.*, 2001, **1**, 207.
- 32 L. Manna, E. C. Scher, L. S. Li and A. P. Alivisatos, *J. Am. Chem. Soc.*, 2002, **124**, 7136.
- 33 P. Reiss, J. Bleuse and A. Pron, *Nano Lett.*, 2002, **2**, 781.
- 34 J. McBride, J. Treadway, L. C. Feldman, S. J. Pennycook and S. J. Rosenthal, *Nano Lett.*, 2006, **6**, 1496.
- 35 M. Nirmal, C. B. Murray and M. G. Bawendi, *Phys. Rev. B*, 1994, **50**, 2293.
- 36 M. Kuno, J. K. Lee, B. O. Dabbousi, F. V. Mikulec and M. G. Bawendi, *J. Chem. Phys.*, 1997, **106**, 9869.

- 37 Y. P. Varshni, *Physica*, 1967, **34**, 149.
- 38 G. Raino, T. Stoferle, I. Moreels, R. Gomes, J. S. Kamal, Z. Hens and R. F. Mahrt, *ACS Nano*, 2011, **5**, 4031.
- 39 L. Malikova, W. Krystek, F. H. Pollak, N. Dai, A. Cavus and M. C. Tamargo, *Phys. Rev. B*, 2006, **54**, 1819.
- 40 D. Valerini, A. Creti, M. Lomasalo, L. Manna, R. Cingolani and M. Anni, *Phys. Rev. B*, 2005, **71**, 235409.
- 41 U. Lunz, J. Kahn, F. Goschenhofer, U. Schussler, S. Einfeldt, C. R. Becker and G. Landwehr, *J. Appl. Phys.*, 1996, **80**, 6861.
- 42 Atoms centered zinc blende structured nanocrystals are formed by adding shells of appropriate atoms as described in P. P. Ingole, G. B. Markad, D. Saraf, L. Tatikondewar, O. Nene, A. Kshirsagar and S. K. Haram, *J. Phys. Chem. C.*, 2013, **117**, 7376, and its Supplementary information. For 2 nm size NCs, replacing 3 shells of Cd atoms by Zn atoms amounts to 24% substitution.
- 43 X. Huang, E. Lindgren and J. R. Chelikowsky, *Phys. Rev. B*, 2005, **71**, 165328.
- 44 S. K. Bhattacharya and A. Kshirsagar, *Eur. Phys. J. D*, 2008, **48**, 355.

**Captions to the Figure:**

**Fig. 1** (Color online) (a) Room temperature optical absorption and (b) PL spectra of alloyed  $Zn_{1-x}Cd_xSe$  NCs recorded with the excitation wavelength 425 nm.

**Fig. 2** (Color online) (a) 10 K PL spectra of alloyed  $Zn_{1-x}Cd_xSe$  NCs recorded with the excitation wavelength 425 nm. (b) Plot depicting change in energy levels with annealing of  $Zn_{1-x}Cd_xSe$  NCs. Shaded area show the energy levels for ZnCdSe-I, and ZnCdSe-Id.

**Fig. 3** (Color online) (a) PL emission intensity as a function of temperature for graded and alloyed NCs. The PL intensity is normalized with respect to 10K intensity of individual sample for comparison. (b) Effect of temperature on emission energy for graded (ZnCdSe-I) and alloyed (ZnCdSe-Id) sample. The data is fitted with varshni equation to obtain quantitative information.

**Fig. 4** (Color online) TRPL spectra of  $Zn_{1-x}Cd_xSe$  NCs, annealed for different time. Diffusion of Zn from shell to core causes the reduction in the life time. The fit to the experimental data is also shown for comparison.

**Fig. 5** (Color online) Partial charge density of HOMO level (a) for core/shell structure [arrangement (i)], (b) graded structure [arrangement (ii)], and (c) Alloy structure [arrangement (iii)], the right panel in figure (c) gives an expanded view of the central region of alloy structure wherein contribution from Zn atoms to HOMO state is highlighted with red circles.

**Fig. 6** (Color online) Total density of states (DOS) as a function of energy relative to respective Fermi energy for three different arrangements studied. The energy levels are split in case of graded and alloyed structures. Consecutive groups of energy states are seen to follow the trend observed experimentally.

Fig. 1

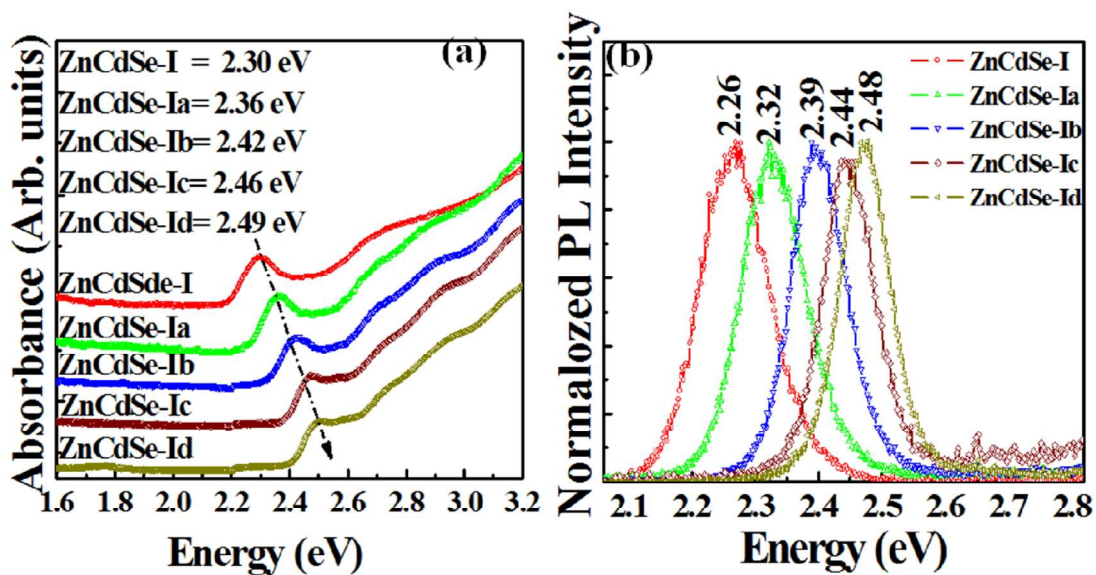


Fig 2

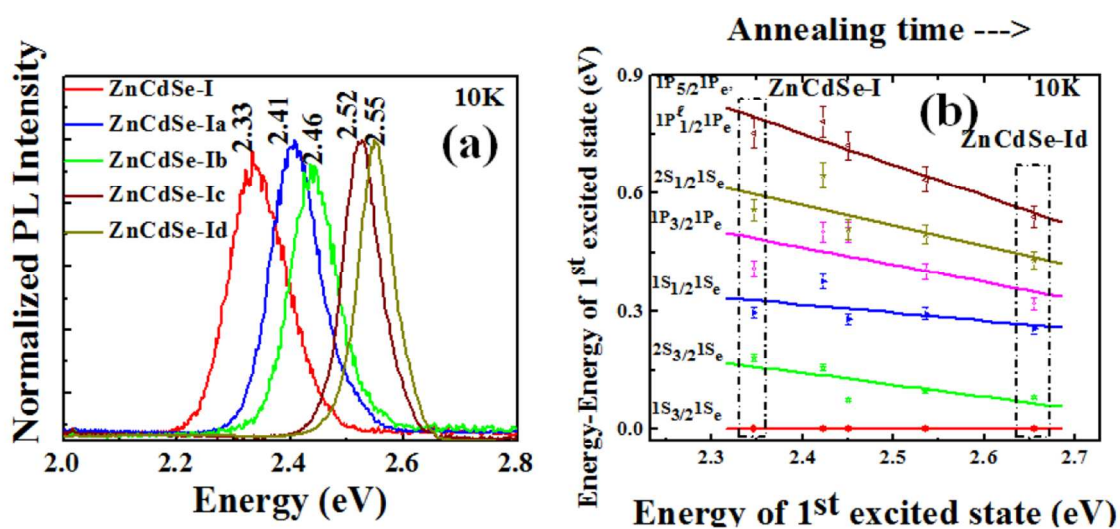


Fig. 3

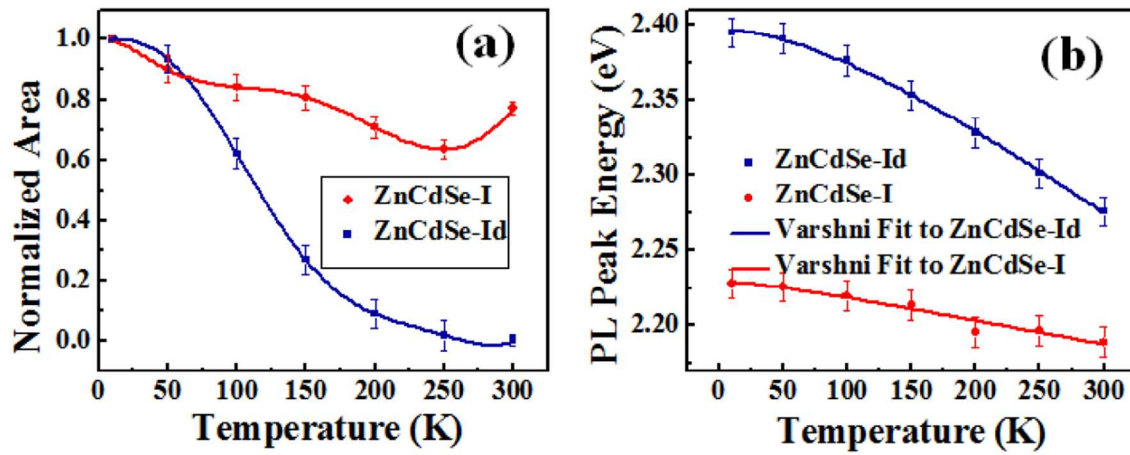


Fig. 4

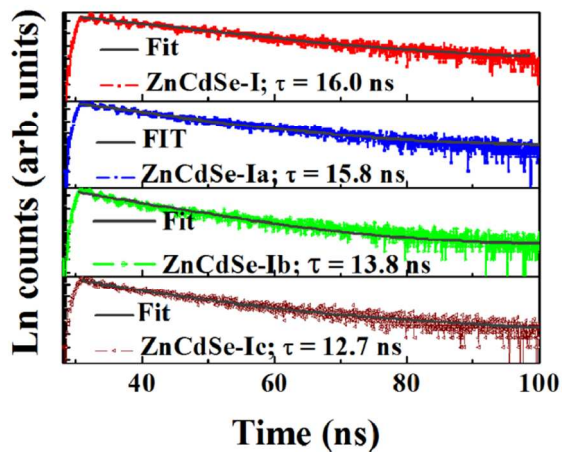


Fig. 5

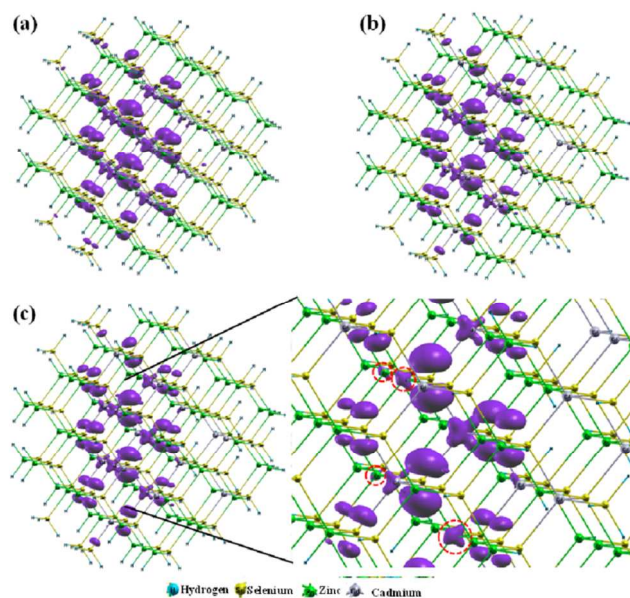
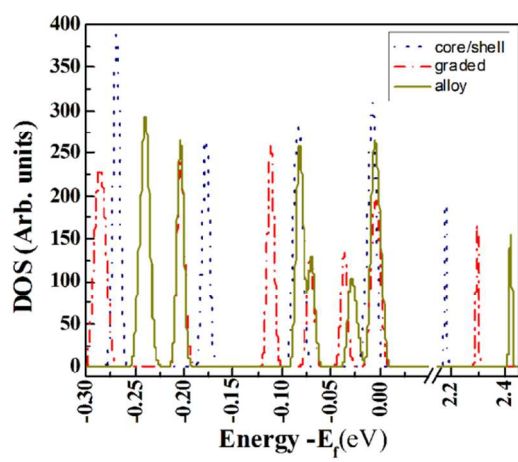
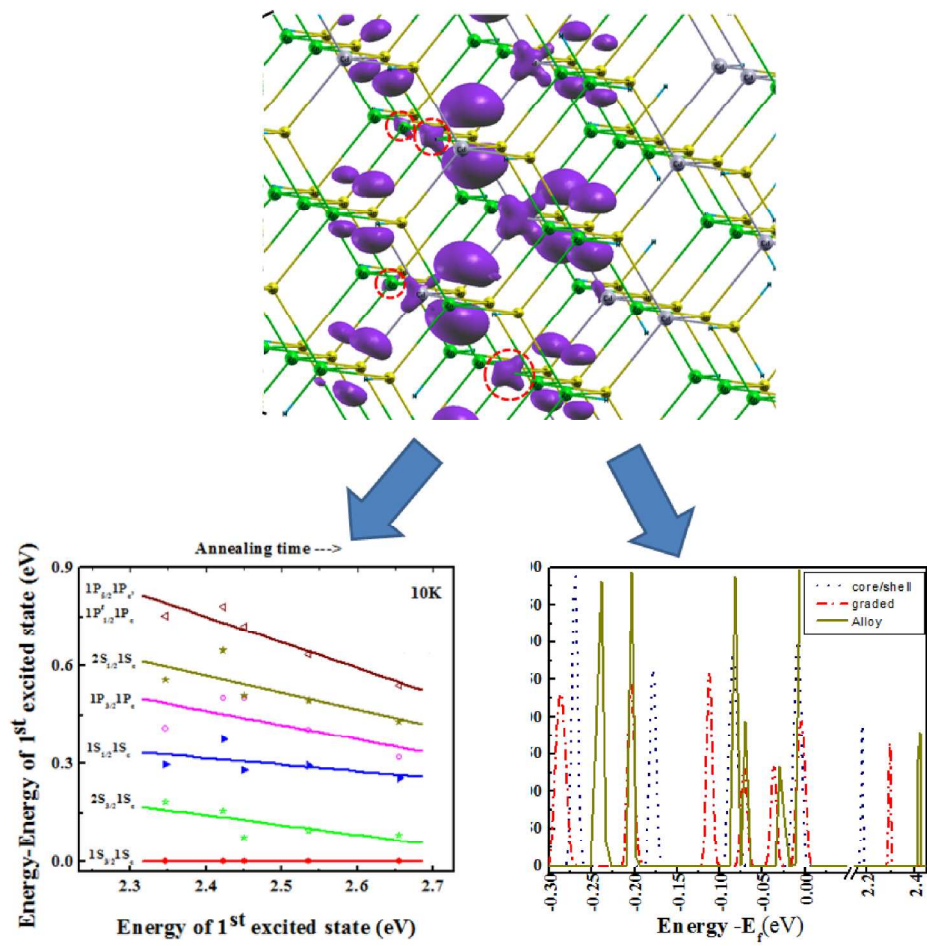


Fig. 6





Hybridization in atomic orbitals opens new way to engineer electronic levels in alloyed NCs  
177x168mm (300 x 300 DPI)